J. Am. Chem. Soc. 1984, 106, 7557-7564

8 sites. It appears that hydrophobic surrounding (in the cavity) has an ordering effect on water molecules, or leads to better formed hydrogen bonds.

(iii) There are 18 flip-flop hydrogen bonds of type O—H··· H—O which might be associated with the disorder of water molecules encountered in this crystal structure. Probably the disorder of water molecules in the β-CD cavities as well as in interstices is the releasing factor. Because flip-flops in a system O—H···O $\rightleftharpoons$ O···H—O represent two energetically near-equivalent states, they are entropically favorable.

(iv) Flip-flops are interconnected to form larger systems. The largest one is an endless flip-flop chain running through the crystal structure (due to the 2_1 screw operation).

(v) The seven interglucose, intramolecular O(2)···O(3) hydrogen bonds in β-CD are all of the flip-flop type. They stabilize the "round" structure of the β-CD macrocycle. Therefore, β-CD adopts the same conformation whether "empty" or filled with guest molecules, in contrast to α-CD which collapses if "empty".

(vi) As observed in the α-CD·6H$_2$O crystal structure, there are again some circularly arranged hydrogen bonds which, in this case, also involve flip-flops.

(vii) Flip-flops can be a general structural feature in starch and in other polymer carbohydrates exhibiting suitably positioned hydroxyl groups. In addition, they will occur in water, and if they are combined with circular hydrogen bonded systems, a dynamical, entropically favorable picture can be envisaged. Flip-flops will also play a role in the hydration of macromolecules, and the β-CD·11H$_2$O crystal structure can be considered as the frozen state of hydrated β-CD.

Acknowledgment. Research sponsored by the Division of Materials Sciences, Office of Basis Energy Sciences, U.S. Department of Energy, under contract W-7405-eng-26 with the Union Carbide Corporation (G.M.B.) and by the Office of Health and Environmental Research, U.S. Department of Energy, under contract W-7405-eng-26 with the Union Carbide Corporation (B.E.H.). C.B. and W.S. gratefully acknowledge support by Bundesministerium für Forschung and Technologie (FKZ 03 B 72 A079), by Deutsche Forschungsgemeinschaft (Sa 196/11-1) and by Fonds der Chemischen Industrie.

Registry No. β-Cyclodextrin undecahydrate, 85490-99-9.

Supplementary Material Available: Tables containing anisotropic temperature factors and structure amplitudes (45 pages). Ordering information is given on any current masthead page.

Stereoelectronic Probes on the Electronic Configuration of Imidyl Radicals: Decompositions of *N*-Bromo-7,8-dichloro-*cis*-bicyclo[4.2.0]octane-*endo*,*cis*-7,8-dicarboximide

Yuan L. Chow* and Yousry M. A. Naguib

Contribution from the Department of Chemistry, Simon Fraser University, Burnaby, British Columbia, Canada V5A 1S6. *Received October 11, 1983*

Abstract: The decomposition of the title *N*-bromide **2** in methylene chloride was investigated by direct photolysis of this compound and by the bromine atom initiated reaction in which two reacting radicals, in addition to bromine atoms, were shown to be involved in the formation of brominated and ring-opened products. The product distribution studies show that both processes lead to the generation of the imidyl radical which undergoes ring opening and intermolecular hydrogen abstraction but does not abstract the endo-C$_3$–H intramolecularly. The Σ electronic configuration was assigned to the imidyl radical. The second radical was generated from the interaction of a bromine atom with **2** but not in the photodecomposition in the presence of bromine atom scavengers. It undergoes intramolecular functionalization at the C$_3$ position specifically but no ring opening reactions. A radical complex of a bromine atom with **2** (or bromine with the imidyl radical) is proposed as the second reacting radical which is simultaneously in equilibrium with *N*-bromide **2** and the imidyl radical. The observed product distributions are rationalized with the equilibria under the reaction conditions. Because the interaction of trichloromethyl radicals as well as bromine atoms with *N*-bromide **2** generates the imidyl radical, this radical is believed to be the ground-state species from energetic considerations.

Introduction

Recent disputes[1-4] over whether one or two succinimidyl radicals serve as the intermediates in NBS decomposition have opened up a new stage of development in this field. While both Skell's[1-3] and Walling's[4] groups agree that two radical species are required to explain the chain propagations, some of their actual experimental data, such as the primary deuterium isotope effects and reaction rate constants, show wide discrepancies. These discrepancies have led to two alternative opinions as to the identity of the two radicals. On the basis of an impressive amount of self-consistent data, Skell's group regarded the two radical chain carriers to be the Π (the ground state) and Σ (the lowest excited state)[2] electronic configuration of the succinimidyl radical; the former operated in NBS–Br$_2$ (or NBS–BrCCl$_3$) and the latter in NBS–olefin systems.[1-3] Contrary to Skell's experimental results, Walling found that the kinetic deuterium isotope effects and the rate constants of rearrangements and hydrogen abstraction were comparable for the two radical species.[4] The latter concluded that only one succinimidyl radical, that of the ground state but not

---

(1) Skell, P. S.; Tlumak, R. L.; Seshadri, S. *J. Am. Chem. Soc.* **1983**, *105*, 5125.

(2) Tlumak, R. L.; Day, J. C.; Slanga, J. P.; Skell, P. S. *J. Am. Chem. Soc.* **1982**, *104*, 7257.

(3) Tlumak, R. L.; Skell, P. S. *J. Am. Chem. Soc.* **1982**, *104*, 7267.

(4) Walling, C.; El-Taliawi, G. M.; Zhao, C. *J. Am. Chem. Soc.* **1983**, *105*, 5119.

0002-7863/84/1506-7557$01.50/0

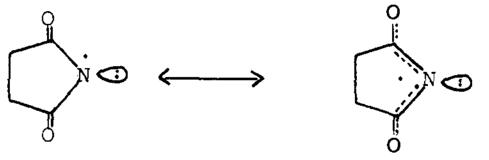

Π electronic configuration

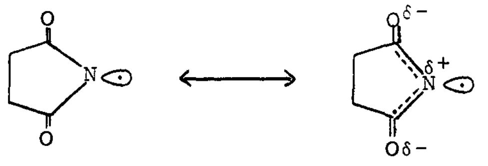

Σ electronic configuration

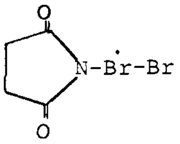

Radical complex

the excited-state radical, was involved in the NBS reactions and that the second radical may be a sort of radical complexes between NBS and a bromine atom.

Our approach was to utilize stereoelectronic probes to examine the geometries involved in hydrogen transfer, from which we hoped to elucidate the electronic configuration of the reacting radical species. The basic principle of the probe is that the orbital containing the unpaired electron and a C–H bond have to be able to approach each other to an interacting distance without an undue molecular strain for efficient hydrogen atom transfer either in intra- or intermolecular mode in which, no doubt, the activation energy for transfer is largely reduced by colinearity of the interacting orbitals.

We have synthesized[5] 7,8-dichloro-*cis*-bicyclo[4.2.0]heptane-*endo,cis*-7,8-dicarboximide (**1**) as the model compound to probe the electronic configuration of the corresponding imidyl radical intermediates. The experimental results of the decomposition of the *N*-bromo imide **2** derived from model compound **1** gave us some insight on the bromination mechanism, from which we wish to clarify the nature of radical intermediates and to draw conclusions on the electronic configuration of the corresponding imidyl radical.

Photodecomposition of 2. The model compound[5] **1** is a sterically crowded molecule which ensures that the cis-fused cyclohexyl and succinimide moieties will react from the exo faces intermolecularly. The cyclohexyl moiety is just as flexible as cyclohexene as shown by the ^{13}C NMR spectrum (five ^{13}C signals) and five ^{1}H NMR signals for the five pairs of magnetically equivalent protons (H_1–H_6, H_{2x}–H_{5x}, H_{3x}–H_{4x}, etc.) showing rapid inversions of the cyclohexyl moiety at the cavity temperature. In a pseudochair conformation, Dreiding models show that the nitrogen and C_3 atoms are separated by ca. 3.05 Å, and in a tucked-in pseudoboat conformation by ca. 2.25 Å. These model studies predict that the endo-C_3–H bond and the nitrogen p orbital (see **4**) are placed in close proximity with a favorable orientation and that the intramolecular hydrogen transfer should occur very efficiently if the radical intermediate has the Π electronic configuration **4**. The inside Br in the radical complex **5** can have dsp^3 hybridization with the trigonal-bipyramid structure to accommodate the un-

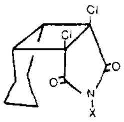

1: X=H
2: X=Br

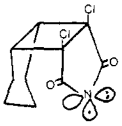

3 (Σ)

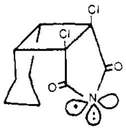

4 (π)

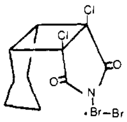

5

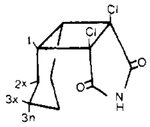

6 (C_1–Br)
7 (C_{2x}–Br)
9 (C_{3n}–Br)
8 (C_{3x}–Br)

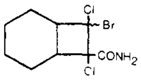

10

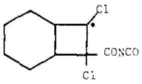

11

paired electron in a basal orbital. Since the distance of endo-C_3–H is only ca. 3.3 and 2.6 Å, respectively, from the Br atom in **2** in the two conformations, the hydrogen atom transfer in **5** no doubt can occur, although the precise geometry of the transition state has not been established. Such intramolecular hydrogen transfer arising from the Π radical **4** and radical complex **5** would lead to specific functionalization to give C_3–Br compounds **8** and **9**. Other possible reactions from the decomposition of **2** are the ring opening of the imidyl radicals to give amides **10** (vide infra) and bromine atom hydrogen abstraction leading to the C-brominated compounds **6**–**9**. The former has been extensively used as evidence of the Σ radical formation in NBS decomposition[1-3] on the basis of orbital symmetry correlations published earlier.[6] Thus in the decomposition of **2** we will rely on analysis of the formation of the C_3–Br **8** and **9** and amides **10**.

Photolysis of *N*-bromide **2** in methylene chloride through a Pyrex filter gave cyclohexyl ring brominated imide **6** (C_1–Br), **7** (C_{2x}–Br), **8** (C_{3x}–Br), and **9** (C_{3n}–Br) in addition to a mixture of two amides **10**: GC analyses of the photolysates always gave a peak for *$CHBrCl_2$* appearing near the methylene chloride peak. The two amides differed in the orientation of the substituents and obviously formed from the ring opening of the imidyl radical to the C-radical **11** which was trapped by a bromine donor to give the corresponding *C*-bromide: this was followed by facile solvolysis and decarboxylation during workup of the product; i.e., **3** (or **4**) → **11** → RCON=C=O → $RCONHCO_2H$ → $RCONH_2$ + CO_2. Indeed, crude products, when obtained by rapid evaporation, showed typical isocyanate absorption at 2280 (s) and 2350 (m) cm^{-1} by IR spectroscopy. The decomposition of **2** did not occur in the dark, and the crude products were stable when kept at room temperature. The *C*-bromides **6**–**9** were also formed by photobromination of imide **1** in which no amides **10** were formed. The amides **10** were more conveniently obtained by photolysis of **2** in the presence of *tert*-butylethylene in which only **1** and **10** were formed. These products were separated by repeated-column and thin-layer chromatography as partially pure samples and identified by their spectroscopic data (see Tables V–VIII under Experimental Section). Two amides **10** showed two closely spaced GC peaks and only one amide was separated in a semipure state. GC-MS unambiguously demonstrated that the two are configurational isomers showing the typical peak pattern of two chlorine and one bromine atoms for the molecular ions.

The structure and stereochemistry of brominated imides **6**–**9** were determined from ^{1}H and ^{13}C NMR spectral analyses and decoupling experiments (Table V and VI) in addition to IR (Table VIII) and mass spectra (Table VII), as described under Experimental Section. The positions of bromine substituents in these imides were assigned from deshielding effects of a bromo substitution[7] on β-carbons by ≈10 ppm in comparison to the parent imide **1**. For example, the bromine in C_{2x}–Br caused the downfield shift of the C_1 and C_3 signals when compared to the ^{13}C signals of **1**; similar examples can be found in Table VI. Extensive decoupling experiments clarified the coupling patterns of the CHBr and some related protons that determined the orientation of the

---

(5) Chow, Y. L.; Naguib, Y. M. A. *J. Chem. Soc., Perkin Trans. 1*, in press.

(6) Koenig, T.; Wielesek, A. *Tetrahedron Lett.* **1975**, 2007.

(7) Stothers, J. B. "Carbon-13 NMR Spectroscopy"; Academic Press: New York, 1972.

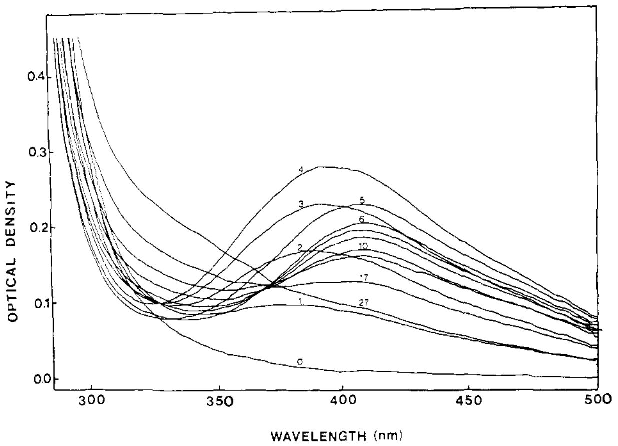

Figure 1. Photolysis of *N*-bromide **2** (8.4×10^{-3} M) in methylene chloride at 22 °C with a 310-nm light ($NiSO_4$ and $CoSO_4$ filter solutions).

bromine substituents and, also, support the assigned bromine positions. From these studies the pseudochair conformation of these *C*-bromides becomes apparent; the C_2 hydrogen of CHBr in C_{2x}–Br assumes the axial orientation and those in C_{3x}–Br and C_{3n}–Br the equatorial and axial orientations, respectively.

Photolysis of *N*-bromide **2** at 310 nm (filter solutions) was monitored with UV spectroscopy as shown in Figure 1. In the 1–4-min irradiation period, the bromine absorption band at 385–395 nm increased, exhibiting an isobestic point at 325 nm. Between 6–12 min of irradiation, this band shifted to 405 nm and decreased slowly with a second isobestic point at 365 nm, indicating that another absorbing species was formed. Further irradiation increased absorbancy in the 320-nm region. Thus, the decreases of the bromine maximum coincided with the formation of more than one species, whose absorptions extended to the 320 nm region. Since similar absorbance was observed in the photobromination of imide **1** with bromine, the absorption might arise from complexes similar to those found in NBS photolysis.[4,8] Visually, the formation of bromine could be detected by the change of a colorless photolysate to light yellow color in several minutes.

The quantum yields of photolysis of *N*-bromide **2** in methylene chloride at various intervals of irradiation were measured by iodometry under the conditions shown in Table II using benzophenone[9] or ferrioxalate[10] actinometry. As the absorptivities of the reacting and actinometry solutions differ widely, the quantum yields in Table I have to be corrected upward. Since the light source is not monochromatic and the absorption spectra fluctuate considerably due to the presence of bromine (see Figure 1), accurate correction factors could not be obtained except in experiment 2 in the presence of *tert*-butylethylene: in this case, a correction factor is estimated to be ca. 30 and the quantum yield would be ca. 40. For other reactions, the correction factors are estimated to be about 20, 5, and 2 for experiments 1, 3, and 4, respectively. Thus, *N*-bromide **2** undergoes photoinitiated chain reactions in the presence of a bromine scavenger with a chain length of about 40, but bromine atom initiated decomposition of **2** has a short chain length of only about 6 (Table I, no. 4). These quantum yield differences also qualitatively agree with the rates of photodecomposition under respective conditions shown in Tables III and IV. Both the complex pattern of the UV absorption and the varying quantum yields suggested that photolysis of **2** changed the reaction pattern as it progresses, most likely owing to the formation of bromine.

Product Distribution Studies. As the bromine atom mediated bromination is an inevitable concurrent reaction,[11] photobromination of imide **1** with bromine in methylene chloride was carried out to determine product distributions. The percentage yields of C_1–, C_{2x}–, and C_3–Br at various ratios of bromine to imide **1** were obtained by GC analysis using benzophenone as the internal standard and given in Table II. The amounts of products were calculated from GC peak areas against the internal standard and their percentage yields were based on the amount of the starting material imide **1**. For either series using a Pyrex filter or a GWV filter (cut off at 380 nm) the ratios C_{2x}–Br/C_1–Br, C_3–Br/C_1–Br, and C_{3x}–Br/C_{3n}–Br are nearly constant regardless of variations in reactant ratios and in product percentages. It should be mentioned that photobromination of methylene chloride under similar conditions is very slow with a quantum yield of about 0.04.

Table I. Quantum Yields of the Photodecomposition of *N*-Bromide **2** in Methylene Chloride

time, min	% decomp	Φ
Irradiation through a Pyrex Filter and by Benzophenone Actinometry[9]		
(1) *N*-Bromide **2** (≈6.3×10^3 M)		
1	6.0	1.95
3	16.8	1.83
5	18.5	1.21
10	31.1	1.01
20	56.7	0.92
(2) in the Presence of *tert*-Butylethylene (0.013 M)		
2	8.2	1.33
4	14.2	1.16
6	23.9	1.30
(3) in the Presence of Bromine (0.66×10^{-3} M)		
1	23.4	7.64
3	60.5	6.57
5	81.7	5.33
Irradiation through GVW filter and by Ferrioxalate Actinomery[10]		
(4) *N*-Bromide **2** (7×10^{-3} M), Bromine (1.3×10^{-3})		
10	27	2.6
30	65	1.9

In view of changing reaction patterns in photodecomposition of *N*-bromide **2**, its product distribution was examined as the function of irradiation durations. Two series of experiments were run at light intensities made different by adjusting the distance of the lamp with similar results. GC analyses of the photolysates in this and subsequent experiments always gave a peak of $CHBrCl_2$ closely placed to the methylene chloride peak in addition to the product peaks. At a low conversion (5–10-min irradiation with 10–15% conversions) the ratios C_{2x}–Br/C_1–Br and C_3–Br/C_1–Br were slightly higher and the C_3–Br/amide ratio was lower than those ratios observed subsequently. The ratios after this initial stage varied very little and were close to those observed in Table III. Throughout the irradiation period, the ratio C_{3x}–Br/C_{3n}–Br was nearly constant at 1.8 ± 0.1. Even at low percentage conversions with relatively higher percentage errors, the trend of the changing reaction pattern could be recognized in the early stage. The results imply that attempts to determine kinetic rate constants of this system will be futile. However, the good reproducibility of the product ratios permits their use as diagnostic tools for mechanistic evaluation.

In Table III, photodecompositions of *N*-bromide **2** at 10^{-3}–10^{-1} M are summarized in experiments 1–6; the reactions were run in methylene chloride through a Pyrex filter to near completion under comparable conditions. In spite of some scattering, the ratios C_{3x}–Br/C_{3n}–Br and C_3–Br/C_1–Br remained nearly constant with the mean values of 1.73 and 3.76, respectively. In contrast, the ratio C_{2x}–Br/C_1–Br increased systematically from 2.2, about that obtained in photobromination of imide **1** (Table II), to 2.9 (ex-

---

(8) Shea, K. J.; Lewis, D. C.; Skell, P. S. *J. Am. Chem. Soc.* **1973**, *95*, 7768.

(9) Hammond, G. S.; Leermaker, S. *J. Phys. Chem.* **1962**, *66*, 1148.

(10) (a) Hatchard, C. G.; Parker, C. A. *Proc. R. Soc. London, Ser. A* **1956**, *518*, 235. (b) Murov, S. L. "Handbook of Photochemistry"; Marcel Dekker: New York, 1973; pp 119–123.

(11) Tanner, D. D.; Ruo, T. C.-S.; Takiguchi, H.; Guillaume, A.; Reed, D. W.; Setiloane, B. P.; Tan, S. L.; Meintzer, C. *J. Org. Chem.* **1983**, *48*, 2743.

Table II. Photobromination of Imide **1** with Bromine[a] in CH_2Cl_2 at 0 °C

	% yields						
$10^3[Br_2]$, M	C_1–Br	C_{2x}–Br	C_{3x}–Br	C_{3n}–Br	$\frac{C_{2x}\text{–Br}}{C_1\text{–Br}}$	$\frac{C_3\text{–Br}^e}{C_1\text{–Br}}$	$\frac{C_{3x}\text{–Br}}{C_{3n}\text{–Br}}$
2.9[b]	1.53	2.75	0.82	0.59	1.80	0.92	1.39
5.9[b]	2.38	4.55	1.20	0.91	1.91	0.89	1.32
12[b]	4.36	8.60	2.30	1.70	1.97	0.92	1.36
6.7[c]	1.97	4.40	1.36	0.83	2.23	1.11	1.64
13[c]	3.96	8.02	2.30	1.46	2.03	0.95	1.58
26[c]	5.27	11.68	3.44	2.18	2.22	1.07	1.58
8.0[d]	1.33	2.53	1.05	0.71	1.90	1.32	1.48

[a] The percentages of **1** were not included. Each photolysate has been analyzed by two or three GC injections and the average values are given; the calculated percentages of errors of means are most <±5% except in a few cases. [b] [**1**] = 10^{-2} M, Pyrex filter; a minor peak (<0.5%) was observed. [c] [**1**] = 2.7×10^{-2} M, GWV filter. [d] Benzoyl peroxide (1.2×10^{-3} M) initiated thermal bromination at [**1**] = 4.2×10^{-2} M at 40 °C. [e] %C_3–Br = %C_{3x}–Br + %C_{3n}–Br.

Table III. Photodecomposition of *N*-Bromide **2** under Various Conditions[a]

		product distribution, %											
expt	$10^2[\mathbf{2}]$, M	**1**	amides	C_1–Br	C_{2x}–Br	C_{3x}–Br	C_{3n}–Br	$(C_3\text{–Br})_e$	$\frac{C_{2x}\text{–Br}}{C_1\text{–Br}}$	$\frac{C_3\text{–Br}}{C_1\text{–Br}}$	$\frac{C_{3x}\text{–Br}}{C_{3n}\text{–Br}}$	$\frac{(C_3\text{–Br})_e}{\text{amides}}$	ref
1	0.47	89	5.15	1.08	2.37	2.71	1.54	3.17	2.19	3.94	1.76	0.62	*b*
2	0.95	81	7.29	1.38	3.09	3.12	1.72	3.46	2.24	3.51	1.81	0.48	*b*
3	1.0	82	8.63	1.51	3.99	3.69	2.48	4.66	2.64	4.09	1.49	0.54	*b*
4	2.4	76	12.13	2.16	5.90	5.42	3.07	6.33	2.73	3.93	1.77	0.52	*b*
5	2.4	71	11.16	2.39	6.32	6.00	3.30	6.91	2.64	3.89	1.82	0.62	*b*
6	9.6	57	13.70	3.34	9.59	7.13	4.07	7.86	2.87	3.35	1.75	0.57	*b*
7	2.5	76	9.39	2.05	5.61	5.07	2.24	5.26	2.74	3.57	2.26	0.56	*c*
8	1.9	63	7.75	2.20	5.71	5.88	2.88	6.56	2.60	3.98	2.04	0.84	*d*
9	1.8	81	6.64	1.21	2.25	2.45	1.25	2.49	1.86	3.06	1.96	0.38	*e*
10	0.95	70	27.0	0	0	0	0	0					*f*
11	1.9	64	27.0	0	0	0	0	0					*c,e,g*
12	2.0	85	11.15	1.81	3.79	1.46	0.98	0.63	2.09	1.35	1.49	0.06	*h*
13	2.9	94	1.0	1.14	4.20	1.44	0.95	1.25	3.68	2.10	1.k2	1.25	*c,i*

[a] All solutions were irradiated through a Pyrex filter at 0 °C to the complete disappearance of *N*-bromide **2**, except experiment 13; all reactions were run in CH_2Cl_2 except experiments 8, 9, and 11. The percentage errors of average values were calculated from two or more GC injections and were in the range of >±5% except in a few cases. $(C_3\text{–Br})_e$ = C_3–Br – C_1–Br; C_3–Br = C_{3x}–Br + C_{3n}–Br. [b] A minor peak (≈0.5 ± 0.1%) was detected. [c] Degassed by freeze–thaw techniques; other experiments used purging with purified nitrogen. [d] CH_2Br_2 as solvent. [e] $CHCl_3$ as solvent; minor peaks (<0.5%) at 5.49 and 10.21 min were detected. [f] Added *tert*-butylethylene, 5×10^{-3} M; the GC showed minor peaks (<3%) at 4.3, 6.3, 7.5, and 9.42 min, none of which were shown to correspond to those of **6**–**9**; the peak for 1,2-dibromo-3,3-dimethylbutane appeared at room temperature 1.8 min. [g] Added $CH_2{=}CCl_2$, 9.9×10^{-2} M; the GC showed minor peaks (<3%) at 2.3, 2.8, 4.6, and 11.18 min, none of these were shown to correspond to those of **6**–**9**. [h] Added ethylene oxide, 0.67 M. [i] Thermally initiated in the presence of benzoyl peroxide, 2×10^{-3} M, at 40 ± 2 °C; a GC peak near the solvent peak was observed.

periment 9) over the 20-fold changes in the concentrations. As this suggests that excess C_{2x}–Br might be formed by a different pathway from that of C_3–Br, we shall leave until later the discussion of its origin. From the C_3–Br/C_1–Br ratios in Tables III and II, it is clear that extra C_3–Br is formed in the photodecomposition of *N*-bromide **2** over C_3–Br formed by bromine photobromination. Assuming that the ratio C_3–Br/C_1–Br by the bromine atom chain in the former photodecomposition is also unity as shown in Table II, the extra C_3–Br formed can be calculated in Table III, namely, $(C_3\text{–Br})_e = (C_3\text{–Br}) - (C_1\text{–Br})$; we assume that $(C_3\text{–Br})_e$ is formed by an intramolecular hydrogen-transfer pathway. The ratios $(C_3\text{–Br})_e$/amides for experiments 1–6 in Table III vary in the range 0.6–0.5. The near constancy of C_3–Br/C_1–Br and $(C_3\text{–Br})_e$/amides in experiments 1–7 indicates that the formation patterns of these types of compounds are nearly parallel to each other.

The results of photodecomposition of *N*-bromide **2** under other conditions are shown in experiments 7–13 in Table III. The product distribution and ratio are very similar when using freeze–thaw cycles for degassing (experiment 7) instead of purified nitrogen gas and are qualitatively indistinguishable when dibromomethane (experiment 8) is used as the solvent instead of methylene chloride. The most important observation is that in the presence of bromine scavengers, such as *tert*-butylethylene or 1,1-dichloroethylene, the photodecomposition of **2** either in methylene chloride or chloroform produced only imide **1** and amides **10** but no *C*-brominated compound (experiments 10 and 11). In chloroform, the photodecomposition of **2** in the absence of dichloroethylene (experiment 9) gives lower percentages of *C*-brominated compounds and amides than those in experiments 1–7 and yields bromotrichloromethane as shown by GC; noteworthy is that $(C_3\text{–Br})_e$ is formed. Therefore, experiments 1–11 unambiguously establish that $(C_3\text{–Br})_e$ is formed only when bromine itself and/or its atoms are present in reaction mixtures.

The photodecomposition of *N*-bromide **2** in the presence of ethylene oxide (experiment 12) and benzoyl peroxide initiated thermal decomposition (experiment 13) are also shown as comparisons. Ethylene oxide reduces, but does not totally eliminate, the bromine formation by scavenging[12] HBr whereby the yields of C-brominated compounds are all reduced in experiment 12; particularly $(C_3\text{–Br})_e$ is drastically diminished, but the amides **10** formation is not affected at all as shown by the significantly decreased ratios C_3–Br/C_1–Br and $(C_3\text{–Br})_e$/amides. The scavenging effect is, therefore, not as efficient as that of olefins in experiments 10 and 11. In the peroxide initiated process, experiment 13, it is obvious that the imidyl radical is not generated efficiently as shown by the low yields of amides **10**: also the extraordinarily high C_{2x}–Br/C_1–Br ratio contrasts with the low C_3–Br/C_1–Br ratio. In this case, the abstracting radical may not be the same as in other experiments.

The results clearly establish that two radical intermediates are involved in the photodecomposition of *N*-bromide **2**. One radical is generated by the chain propagation and photoexcitation of **2** when molecular bromine and atomic bromine are scavenged. As this radical leads to the formation of amides **10**, it can be safely assigned to an imidyl radical. The other radical is generated only when bromine atoms and/or bromine are not scavenged and undergoes intramolecular hydrogen transfer leading to the formation of $(C_3\text{–Br})_e$ as shown in experiments 1–9; in particular, the incomplete scavenging in experiment 12 provides pertinent data to relate to the limiting cases (experiments 10 and 11) and

---

(12) Lu, F. L.; Naguib, Y. M. A.; Kitadani, M.; Chow, Y. L. *Can. J. Chem.* **1979**, *57*, 1967.

Table IV. Photolysis of *N*-Bromide **2** and Bromine through a GWV Filter[a]

		product distribution, %							$\frac{C_{2x}\text{–}Br}{C_1\text{–}Br}$	$\frac{C_3\text{–}Br}{C_1\text{–}Br}$	$\frac{C_{3x}\text{–}Br}{C_{3n}\text{–}Br}$	$\frac{(C_3\text{–}Br)_e}{\text{amides}}$
expt	$10^3[Br_2]$, M	**1**	amides	C_1–Br	C_{2x}–Br	C_{3x}–Br	C_{3n}–Br	$(C_3\text{–}Br)_e$				
14	0	88	4.41	2.27	4.90	2.90	2.21	2.84	2.16	2.25	1.31	0.64
15	0.77	81	3.51	2.90	7.00	3.25	2.25	2.60	2.41	1.90	1.44	0.74
16	3.1	75	1.15	4.07	9.31	3.68	2.07	1.68	2.29	1.41	1.78	1.46
17	6.2	72	0.61	4.97	11.43	4.29	2.32	1.64	2.30	1.33	1.85	2.69
18	12	65	0.27	6.80	15.92	5.73	3.22	2.15	2.34	1.32	1.78	7.96
19	92	55	0.0	10.30	22.75	7.25	4.07	1.02	2.21	1.10	1.78	–

[a] The concentration of **2** was (9.5 ± 0.1) × 10^{-3} M except experiment 14 in which it was 9.2 × 10^{-3} M. The experiments were run to >90% disappearance of **2**. The percent errors of the mean values of more than two injections were shown to be <±5% except in a few cases. C_3–Br = C_{3x}–Br + C_{3n}–Br; $(C_3\text{–}Br)_e$ = C_3–Br – C_1–Br.

support our claims. Thus the two radicals in addition to bromine atoms are the chain carriers in experiments 1–9, but the second radical does not lead to the amide formation as shown below.

Bromine Atom Initiated Decompositions of 2. The photodecomposition of *N*-bromide **2** in methylene chloride through a GWV filter (cut off <380 nm, Table IV, experiment 14) was very slow since **2** absorbs very weakly above 360 nm (at 10^{-1} M) and the initiation depends on a trace amount of bromine in the solution. While the product distribution shows that amides **10** decrease drastically and C-brominated compounds increase, the $(C_3\text{–}Br)_e$/amide ratio remained the same in comparison to experiments 1–7 which used a Pyrex filter. Similar photolysis in the presence of increasing amounts of added bromine (experiments 14–19) showed that while the ratios C_{2x}–Br/C_1–Br remained relatively unchanged, C_3–Br/C_1–Br decreased systematically, approaching a nearly unity ratio obtained in the photobromination of imide **1** by bromine (bromine atom mechanism). Three series of similar experiments were carried out with a 100-fold variation of bromine concentrations (10^{-3}–10^{-1} M) in which the light absorptivity of the solutions changed from 0.2 to >1 showing the same trend as the data given in Table IV. As the bromine concentrations in these experiments are higher than $^1/_{10}$ of the *N*-bromide concentration, bromine must be the C-radical scavenging agent because bromine is about 1000 times more reactive than NBS,[13] which is, in turn, more reactive than *N*-bromide **2** for steric reasons.

Therefore, the propagation step involves only the regeneration of bromine atoms in experiments 15–19, and amides **10** (therefore, the imidyl radical) in these experiments must be generated by another route, namely, by the interaction of bromine atoms with **2**. The steady increases in the C-brominated compounds contrasted with the drastic decreases in amides **10**. They showed that the bromine atom chain process gradually dominated the reaction pattern as bromine concentration increased. Yet, in reality, the calculated $(C_3\text{–}Br)_e$ also decreased, but C_3–Br/amides increased rapidly with increasing bromine concentrations. This indicates that the imidyl radical responsible for the formation of amides **10** is intercepted by bromine to form the second radical responsible for the $(C_3\text{–}Br)_e$ formation; e.g., amides **10** are not formed from the second radical intermediate. Therefore, it is concluded that *the thermal interaction of bromine atoms with N-bromide* ***2*** *generates both the imidyl radical and the second radical intermediate* and that the rates of their formations depend on bromine and/or bromine atom concentrations.

The Nature of the Two Radicals. For the limiting cases where bromine and/or bromine atoms are entirely or partially scavenged (experiments 10–12), the chain carrier in the propagation processes is the imidyl radical **3** according to a well-established mechanism[1-3] as shown below, where R· represents the C radicals obtained from the ring opening and hydrogen abstraction.

$$\underset{\mathbf{2}}{Ac_2NBr} \xrightarrow{h\nu} \underset{\mathbf{3}}{Ac_2N\cdot} + Br\cdot \tag{1}$$

$$\underset{\mathbf{3}}{Ac_2N\cdot} \rightarrow R\cdot \tag{2}$$

$$R\cdot + \underset{\mathbf{2}}{Ac_2NBr} \rightarrow RBr + \underset{\mathbf{3}}{Ac_2N\cdot} \tag{3}$$

Since the imidyl radical is generated not only by the thermal interactions of C radicals with *N*-bromide **2** but also by those of the $Cl_3C\cdot$ and bromine atom, energetic considerations predict that the imidyl radical is more likely to be in the ground state instead of the lowest excited state. With acceptance of the reactions of bromine atoms with *N*-bromo linkages as thermoneutral,[3] generation of the excited-state imidyl radicals from these reactions would be highly endothermic if one assumes the ground-excited-state energy gap is 15–20 kcal/mol.[3,6,14,15] The size of the energy gap also suggests that, if the excited state imidyl radical is generated, its internal conversion to the ground state would be fast and the lifetime of the excited state will be very short.[16] *The ground-state imidyl radical must have the Σ electronic configuration as in* ***3*** *since it fails to intramolecularly abstract the endo-C_3 hydrogen.* This conclusion is neither in full agreement with Skell's proposal nor with several theoretical calculations that the Σ radical is the excited-state radical.

Discussion on the nature of the second radical must consider a number of conclusions arrived at in the previous sections, namely, (i) it is generated by the thermal interaction of a bromine atom with *N*-bromide **2** in which the imidyl radical **3** is also formed concurrently *albeit* inefficiently, (ii) it is probably formed by the interaction of bromine and the imidyl radical **3**, (iii) it is not formed from the photodecomposition of **2** in the presence of bromine and bromine atom scavengers, (iv) it is responsible for the formation of $(C_3\text{–}Br)_e$ by intramolecular hydrogen transfer, and (v) it fails to open the imide ring to give amides **10**.

Conclusions iv and v are apparently consistent with the Π-imidyl radical configuration **4**, an orbital isomer[13] of the Σ-imidyl radical **3** for the second radical: indeed the latter conclusion has been extensively used as a criterion for Π radical formations by Skell's group.[1-3] However, the assignment of the Π radical configuration to the second radical fails to satisfy the following arguments and, therefore, the idea has been abandoned. First, even if the concurrent generations of both Σ and Π radicals (ground- and excited-state species) from the singular interaction of a bromine atom with *N*-bromide **2** are feasible, their proportions must be independent of the reactant concentrations; that is, the ratio $(C_3\text{–}Br)_e$/amides in Table IV should not change drastically with rapid increases in the concentrations of photogenerated bromine atoms in experiments 15–17. Second, from stereochemical points of view, the intramolecular hydrogen transfer[17,18] in the Π radical **4** should be very efficient (vide supra), and one should observe a rapid increase in $(C_3\text{–}Br)_e$, at least in the low concentration range of added bromine, in contrast to the results obtained in Table IV. Finally, experiment 11 is designed to generate the Π radical **4** according to Skell's recipe ($CHCl_3$, $CCl_2{=}CH_2$)[3] assuming the dividing line for Σ–Π radical generations is similar to that of the

---

[13] Skell, P. S.; Tuleen, D. L.; Readio, P. D. *J. Am. Chem. Soc.* **1963**, *85*, 3134.

[14] Denver, M. J. S.; Pakiari, A. H.; Pierini, A. B. *J. Am. Chem. Soc.* **1982**, *104*, 3242.

[15] Apeloig, Y.; Schreiber, R. *J. Am. Chem. Soc.* **1980**, *102*, 6144. Clark, T. R. *J. Am. Chem. Soc.* **1979**, *101*, 7446.

[16] Turro, N. J. "Modern Molecular Photochemistry"; The Benjamin: Menlo Park, CA, 1978; Chapter 3.

[17] Joseph, T. C.; Tam, J. N. S.; Kitadani, M.; Chow, Y. L. *Can. J. Chem.* **1976**, *54*, 377. Akhtar, M. *Adv. Photochem.* **1964**, *2*, 263.

[18] (a) Scheffer, J. R. *Acc. Chem. Res.* **1980**, *13*, 283. (b) Appel, W. K.; Jiang, Z. Q.; Scheffer, J. R.; Walsh, L. *J. Am. Chem. Soc.* **1983**, *105*, 5354.

succinimidyl radicals.[3] The results are strictly compatible with the exclusive formation of the E radical **3** but not with that of the Π radical. In this regard, both Walling's and Tanner's groups also reported that the conditions were not specific to generating the Π succinimidyl radical since β-bromopropionyl isocyanate was formed substantially in NBS decompositions.[4,11]

The conclusions i, ii, and iii lead us to assign radical complex **5** to the second radical. Furthermore, the constancy of the $(C_3{-}Br)_e$/amides ratios in experiments 1–7 under similar photolysis conditions leads us to propose that the reacting radicals **3**, **5**, and Br· are related by a series of equilibria as shown in eq 5 which

$$\mathrm{Br}^2 \xrightarrow{h\nu} 2\mathrm{Br}\cdot \tag{4}$$

$$\mathrm{Br}\cdot + \underset{\mathbf{2}}{(\mathrm{Ac})_2\mathrm{NBr}} \rightleftarrows \underset{\mathbf{5}}{(\mathrm{Ac})_2\mathrm{N\dot{B}rBr}} \rightleftarrows \mathrm{Br}_2 + \underset{\mathbf{3}}{\mathrm{Ac}_2\mathrm{N}\cdot} \tag{5}$$

$$\underset{\mathbf{5}}{\mathrm{Ac}_2\mathrm{N\dot{B}rBr}} + \mathrm{RH} \rightarrow \mathrm{Ac}_2\mathrm{NH} + \cdot\mathrm{Br} + \mathrm{RBr} \tag{6}$$

$$\mathrm{Br}\cdot + \mathrm{RH} \rightarrow \mathrm{HBr} + \mathrm{R}\cdot \tag{7}$$

$$\underset{\mathbf{3}}{\mathrm{Ac}_2\mathrm{N}\cdot} + \mathrm{RH} \rightarrow \mathrm{Ac}_2\mathrm{NH} + \mathrm{R}\cdot \tag{8}$$

$$\mathrm{R}\cdot + \mathrm{Br}_2 \rightarrow \mathrm{RBr} + \mathrm{Br}\cdot \tag{9}$$

must be set up much more rapidly than the subsequent hydrogen abstraction (eq 6–8) and rearrangement (eq 2).[19] Since the reaction of Br· and *N*-bromide is nearly thermoneutral,[3] the reverse reaction, i.e., the reaction of bromine with imidyl radicals, can also occur on the basis of microscopic reversibility. The proposal also implies that the radical complex **5** is sufficiently long-lived that it acts as the second radical intermediate in analogy to $\mathrm{Ar\dot{I}Cl}$ radical behavior.[20] An overall reaction pattern of hydrogen abstraction by **5** is represented by Equation 6, which may be viewed as an imidyl radical reaction modified by bromine: the bromine atom is essentially a catalyst.

The proposal can explain the observed data without an assumption of excited state radical reactions. If the substrate contains allylic hydrogen, the bromine atom chain process dominates[21] and the equilibrium shifts to the left. As shown in experiments 14–17, at low concentrations of bromine, the imidyl radical **3** is still generated by bromine atom initiation. As the bromine concentration increases, **3** is rapidly trapped by bromine and the equilibrium shifts to the left, leading to drastic diminutions in the imidyl radical reactions as in experiments 17–19. Under constant illumination of *N*-bromide **2**, the concentrations of all radical species Br·, **3**, and **5** are proportionately upgraded by the interconnecting equilibria as the concentration of *N*-bromide **2** increases (Table III). Consequently the radicals react in nearly the same proportion regardless of the concentration of **2** to give almost constant values of $(C_3{-}Br)_e$/amides as shown in experiments 1–6. Naturally when bromine and its atoms are scavenged, the equilibrium shifts far to the right (experiments 10 and 11), to show just the reaction pattern of **3**.

Since both $C_{3x}{-}Br$ and $C_{3n}{-}Br$ are derived from the reaction of the C_3 radical with bromine transfer agents, the constancy of their ratio in Tables II, III (experiments 1–6), and IV must mean that, in each set of conditions, the same transfer agent(s) is involved. The close agreement of the ratio $C_{3x}{-}Br/C_{3n}{-}Br$ in Tables III (experiments 1–6) and IV, except a few scatters, may be taken as an indication that bromine is the major trapping agent for the C radicals in both systems (eq 9).

The small but systematic rise in $C_{2x}{-}Br/C_1{-}Br$ ratios in Table III above that observed in photobromination of imide **1** (Table II) is dependent on the concentration of **2**. Clearly, the extra $C_{2x}{-}Br$ cannot be formed from the action of the imidyl radical **3** (see experiments 10 and 11) or bromine atom. At this stage, we tentatively propose that the extra $C_{2x}{-}Br$ is formed from intermolecular hydrogen abstraction by the radical complex **5** on **1** and **2**. Since **5** is a sterically hindered radical, it should abstract hydrogen selectively from relatively unhindered sites. Yet we cannot provide a satisfactory rationalization as to why the $C_2{-}H$ should be preferentially abstracted. The formation of the extra $C_{2x}{-}Br$ is very prominent in benzoyl peroxide initiated decomposition (experiment 13) and probably not related to that of $(C_3{-}Br)_e$ and amides **10** (vide supra) and does not affect the discussion presented above.

Discussion

In analogy to the NBS decomposition pattern,[1-4] the decomposition of *N*-bromide **2**, initiated either by light or by radicals, involves two reactive radical species in addition to bromine atoms as chain carriers. One of them can be unambiguously assigned to the Σ-imidyl radical **3** on the basis of its failure to abstract hydrogen intramolecularly and its ring opening to **11**. The significant departure from the interpretation in the NBS decomposition is the assignment of the second reactive radical to the radical complex **5** which is formed either by the trapping of bromine atoms or the imidyl radical **3** as shown in eq 5. We have been forced to abandon the Π-imidyl radical **4** as an alternative for the second radical on the basis of kinetic, stereochemical, and energetic considerations; the same arguments are clearly in favor of radical complex **5**. As the interaction of bromine atoms with *N*-bromide is energetically unfavorable for generating an excited-state imidyl radical, the Σ-radical configuration **3** must be the ground state; this is another major disagreement with the current proposal on succinimidyl radicals, particularly with theoretical studies.[6,14,15]

These discrepancies may be interpreted by two different approaches. First of all they may arise from the inductive effects associated with the presence of two chlorine substituents at the α- and α′-positions and the ring strains associated with the tricyclic imidyl radical system **3** and **4**. This speculation may be examined by decomposition studies of other model compounds and by further theoretical studies. Such studies of imidyl radical chemistry will no doubt be more fruitful if *N*-bromides are not used, so that complications from bromine atom chemistry can be eliminated. Secondly, on the basis of speculation described below, the Σ–Π states may have a very small energy gap, say <5 kcal/mol, and may interconvert rapidly enough that the ring opening occurs from the appropriate electronic state. This interpretation, however, is not likely since it requires that the ring-opening reaction demands about the same activation energy as intermolecular hydrogen transfer does but much less than intramolecular hydrogen transfer.

Is the ground state of imidyl radicals likely to have the Σ electronic configuration? That is, can the E configuration be more stable than the Π configuration? For amidyl radicals, it has been shown by chemical methods,[16,22] ^{13}C CIDNP,[23] and ESR[24] techniques that the radical intermediates possess the Π electronic configuration which is the ground state as opposed to the excited state of the Σ electronic configuration. Simple molecular orbital theory dictates that two electrons in the sp^2 orbital (the Π radical assuming sp^2 configuration at the nitrogen center: see the structures in the Introduction) would possess a lower potential energy than two electrons in the p orbital (therefore, one electron in the sp^2 orbital for the E radical). Naturally, one-electron delocalization with the carbonyl group in the Π electronic configuration vs. two-electron resonance in Σ electronic configuration has to be considered; no doubt, the latter is larger than the former. In amidyl radicals, such delocalization gains with one carbonyl group are not big enough to offset the sp^2–p orbital energy split. Therefore, amidyl radicals are expected and have been shown to have the Π electronic configuration. For imidyl radicals with the two carbonyl group conjugation, the delocalization gain for the

---

[19] Chow, Y. L.; Naguib, Y. M. A. *Rev. Chem. Intermed.*, in press.

[20] Breslow, R.; Corcoran, R. J.; Snider, B. B.; Doll, R. J.; Khanna, P. L.; Kaleya, R. J. *J. Am. Chem. Soc.* **1977**, *99*, 905.

[21] For example, the $\Delta^{2,3}$ analogue corresponding to *N*-bromide **2** was photolyzed to give primarily the C_4-brominated (allylic bromination) olefinic imide: the product analyses showed that this compound was formed mainly by the bromine atom chain reaction.

[22] Lessard, J.; Mondon, M.; Touchard, D. *Can. J. Chem.* **1981**, *59*, 431.

[23] Brown, C.; Lawson, A. J. *Tetrahedron Lett.* **1975**, 191.

[24] Sutcliff, R.; Griller, D.; Lessard, J.; Ingold, K. U. *J. Am. Chem. Soc.* **1981**, *103*, 624.

Σ electronic configuration over the Π electronic configuration can be very substantial to place the former at a lower energy level. Therefore, the Σ electronic configuration can be the ground state of imidyl radicals. Indeed, such a possibility was proposed in 1967 by similar arguments.[25]

Experimental Section

General Conditions. Unless specified otherwise, the following experimental conditions were used. Infrared spectra were recorded with a Perkin-Elmer 599B spectrometer using Nujol mulls. Ultraviolet spectra were obtained on a Cary 210 spectrometer. Mass spectra and gas chromatography-mass spectra were taken with a Hewlett-Packard 5985 mass spectrometer using a SE-30 capillary column. Nuclear magnetic resonance spectra were recorded at 400 MHz on a Bruker WH400 spectrometer in the FT mode, and an internal lock (deuterium) was used. The chemical shifts in ^{1}H NMR spectra were referred to the solvent signals (δ 7.24, 7.15, and 2.04 for $CDCl_3$, C_6D_6, and acetone-d_6, respectively. The peak positions of ^{13}C signals were measured relative to the solvent signal. Separations by column chromatography were carried out on silica gel (Baker, 60–200 mesh).

Chemicals. Dichloromethane (Fisher, spectroanalyzed grade) was purified by either distillation over P_2O_5 or successive extraction with concentrated H_2SO_4, distilled water, and 5% aqueous sodium bicarbonate, drying over anhydrous calcium chloride, and distillation over P_2O_5. GC analysis showed dichloromethane, purified by either method, to be 99.9% and contained a trace of carbon tetrachloride. Dibromomethane (Eastman Kodak) and chloroform (Burdick and Jackson) were distilled over P_2O_5 when they were needed. GC analysis showed them to be 99.8%. Bromine (Fisher) was used as supplied; 3,3-dimethyl-1-butene (Aldrich) and 1,1-dichloroethylene were distilled prior to experiments. Commercial nitrogen (Union Carbide Linde, 99.997%) was scrabbed with a train of Fieser's solution, concentrated H_2SO_4, and KOH pellets.

Preparation of *N*-Bromide 2. *tert*-Butyl hypobromite in CCl_4 (1–1.2 mol equiv)[17] was added in the dark to the stirred dichloromethane solution of imide[5] **1** kept at ca. −15 °C. After 45 min, the solvents were removed under vacuum. The resulting white solid was washed with cyclohexane and dried over P_2O_5 under vacuum. *N*-Bromo-7,8-dichloro-*cis*-bicyclo[4.2.0]octane-*endo*,*cis*-7,8-dicarboximide (**2**) was obtained in 82%: mp 128–129 °C; UV λ 260 nm ($\epsilon \approx 240$ tailing to 360 nm) in CH_2Cl_2; IR 1340 (s), 1300 (m), 1190 (s), 1135 (s), 950 (w), 875 (m), 810 (m), 710 (m) cm^{-1}; ^{1}H NMR ($CDCl_3$ at 60 MHz) δ 1.2–2.1 (m, 8 H), 3.15 (m, 2 H). The purity of *N*-bromide **2** used in the photolysis was assumed to be ≥95% since no parent imide could be detected by ^{1}H NMR and IR spectroscopy. Iodimetric titration showed the *N*-bromide **2** to be 97% pure, which was kept in a dark desiccator over P_2O_5.

General Procedure of Photodecomposition of 2. In a Pyrex photocell of either ca. 8- or 40-mL capacity, an appropriate solution of *N*-bromide **2** was purged with purified nitrogen for a few minutes. The photocell was kept in a water bath (2 ± 2 °C) and about 2 in. from the light source: the latter was either a 450-W medium-pressure mercury lamp without a filter or a 200-W one placed in a GWV filter (cut off at 380 nm), both of which were placed in a water-cooled cold finger. At intervals, small samples were taken for KI-starch paper tests. When the test was feeble or negative, a sample of the photolysate was filtered through a short pad of silica gel which was washed with methylene chloride containing 5% methanol. To the combined methylene chloride solution was added a measured amount of the standard solution and the total solution was analyzed by GC. Some of the photolysates were evaporated, and the crude products were examined by IR spectroscopy to show strong absorptions at 2280 (s) and 2350 (m) cm^{-1}.

GC-MS of the photolysates always showed a $CHBrCl_2$ peak (room temperature ≈0.6 min) after the methylene chloride peak: mass spectrum, *m/e* (%) 168 (0.4), 166 (1.4), 164 (3), 162 (2), 131 (8), 129 (35), 127 (21), 8.5 (68), 83 (100).

Two types of controls were carried out. A preanalyzed photolysate was irradiated further for 3 h: at each hour interval, the GC analysis showed that the product distributions were identical. Second, a photolysate was evaporated; the crude product was added with a definite amount of a solution containing the standard (benzophenone). GC analysis of the solutions before and after passing through a short column of silica gel and washings gave identical results.

GC analyses were carried out with a Hewlett-Packard 5792A equipped with a HP3990 integrator and an OV-1 capillary column (HP 12.5 × 0.20 mm). The response curve of the standard (benzophenone) to imide **1** were determined first. The correction factors of the products **6**–**10** were assumed to be the same with this curve. From each peak, the absolute yields of the compounds were calculated from the response curve. The percentage yields were calculated on the basis of millimoles of **2** used. In each analysis, more than two injections were made, and the peak areas were averaged to calculate the absolute yields of these products. A typical set of the retention times were 8.2 (imide **1**), 8.5 and 8.7 (amides **10**), 14.8 (C_1–Br), 16.25 (C_{2x}–Br), 17.8 (C_{3x}–Br), and 18.2 min (C_{3n}–Br).

The reactions carried out to less than 100% decomposition of *N*-bromide **2** were successively treated with 5% aqueous sodium bisulfite and 5% sodium bicarbonate. The aqueous solution was extracted with methylene chloride. The combined methylene chloride extracts were dried over Na_2SO_4 and analyzed by GC after the addition of a standard solution.

Irradiation of **2** in the presence of bromine was carried out with a 200-W Hanovia lamp filtered through a GWV filter. The sample was treated with a small amount of cyclohexene to discharge the color and tested with a KI–starch paper. The solution reacted acidic to a litmus paper test. The workup and analysis were the same as that shown above.

A CH_2Cl_2 solution of **2** kept at 0 °C in the dark showed no change in the IR and NMR spectra.

Photolysis in the presence of 1,1-dichloroethylene (experiment 11) was carried out to the complete disappearance of **2**. The usual workup and GC analysis (isothermal at 200 °C at 12 psi of He) gave imide (room temperature 5.66 min, 1.8 × 10^{-2} mmol) and amides (room temperature 6.11 and 6.30 min, 7.5 × 10^{-3} mmol) in addition to the unidentified minor peaks at 0.5 (1.5%), 2.3 (3%), 2.8 (1%), 4.6 (1%), and 11.18 min (3%). Under the same GC conditions, the retention times of a product mixture were 5.63 (imide), 5.95 and 6.27 (amides), 10.91 (C_1–Br), 12.11 (C_{2x}–Br), 13.38 (C_{3x}–Br), and 13.63 min (C_{3n}–Br). Photolysis in the presence of neohexene (experiment 10) was carried out and analyzed in a similar manner, its minor peaks were confirmed to be other than those of **6**–**9**.

Benzoyl Peroxide Initiated Decomposition of 2 in Methylene Chloride. The methylene chloride (1.5 mL) solution of benzoyl peroxide (2 × 10^{-3} M) and **2** (14.1 mg, 0.043 mmol) was degassed by three freeze–thaw cycles. The sealed tube was kept at 40 ± 2 °C for 24 h in a dark place. The solution, which showed positive KI–starch paper tests, was washed successively with 5% sodium bisulfite, 5% sodium bicarbonate, and water. Workup in the usual manner gave the GC result shown in experiment 13.

Photobromination of Imide 1. Imide **1** (230 mg, 0.9 mmol) and bromine (1.4 mmol) in methylene chloride (20 mL) were irradiated with a 450-W lamp at 0 °C for 6 h. More bromine (1.8 mmol in 5 mL of CH_2Cl_2) was added and irradiation continued for another 4 h. The photolysate was washed with 5% sodium bisulfite and 5% sodium bicarbonate. The usual workup of the organic layer gave an oil, which was chromatographed on silica gel. Elution with 5% EtOAc in hexane gave a fraction (7.7 mg) which was recrystallized from methylene chloride to afford C_{3n}–Br **8** contaminated with a small amount of **1**. Elution with 10% EtOAc in hexane afforded imide **1** (62 mg). Elution with 20% EtOAc in hexane gave a fraction (47 mg), which was purified by preparative TLC to give a mixture of C_1–Br **6** and C_{2x}–Br **7** in 1:1 ratio.

Photolysis of *N*-Bromide 2. A solution of **2** (340 mg, 1.05 mmol) in methylene chloride (40 mL) was irradiated until KI–starch paper test was negative and worked up as above. The oil was chromatographed on silica gel. Elution with 10% ether in petroleum ether gave imide **1** (164 mg) contaminated with C_{3n}–Br. Elution with 10–20% ether in petroleum ether gave fractions A (28 mg), B (59 mg), and C (31 mg). Fraction A was recrystallized to give the slower moving amide (>90%) contaminated by the other amide. Fraction B, by preparative TLC on silica gel and EtOAc–petroleum ether, afforded a solid which was recrystallized from methylene chloride to give C_{2x}–Br **7** contaminated by **1** (8%) and **6** (5%) as shown by GC analysis. Fraction C was recrystallized from methylene chloride several times to give C_{3x}–Br **8** contaminated with trace amounts of **1** (9%) and **6** shown by GC analysis. These semipure samples were used to record the ^{1}H (4%) and ^{13}C NMR (Table V and VI), IR (Table VII), and mass spectral data (Table VIII).

Decoupling and NOE Experiments. C_{3x}–Br **8**: Irradiation of the C_3–H (4.32 ppm) caused the C_2–H and $C_{2'}$–H to collapse to double doublets but no change in the C_1–H and C_6–H. Irradiation of C_1–H (3.38 ppm) caused C_2–H and $C_{2'}$–H to collapse to double doublets, but that of C_6–H (3.27 ppm) caused no change in C_2–H, $C_{2'}$–H, and C_3–H.

C_{3n}–Br **9**: Irradiation of the C_3–H (3.78 ppm) caused a C_2–H to collapse to a double doublet but no change in C_1–H and C_6–H. Irradiation of the C_1–H and C_6–H (3.16 ppm) caused a C_2–H to collapse to a double doublet but no change in C_3–H. Upon irradiation of the C_3–H (3.78 ppm), the C_1–H and C_6–H (3.16 ppm) intensity was enhanced by 5.7%; a similar experiment with C_{3x}–Br did not show enhancement.

C_{2x}–Br **7**: Irradiation of C_2–H (4.22 ppm) caused the C_1–H to collapse to a doublet but no change in the C_6–H.

---

[25] Hedaya, E.; Hinman, R. L.; Schomaker, U.; Theodoropulas, S.; Kyle, L. M. *J. Am. Chem. Soc.* **1967**, *89*, 4875.

Table V. ^{1}H NMR Parameters[a]

compd	chemical shifts, ppm	coupling constants (Hz)
C_{2x}–Br **7**	1.45 (m, 3 H), 1.77 (m, 1 H), 1.88 (m, 1 H), 1.98 (m, 1 H), 3.3 (td, 8.2, 11.8, H_6), 3.53 (dd, 8.0, 12, H_1), 4.22 (ddd, 4.5, 7.8, 9.0, H_2)	$J_{1,2}$ (8.0), $J_{1,6}$ (12), $J_{2,3}$ (4.5), $J_{2,3'}$ (9), $J_{6,5}$ (8.2), $J_{6,5'}$ (8.2)
C_1–Br[b] **6**	2.33 (td, 3.6, 15.1, H_2), 3.44 (t, 8.0, H_6)	$J_{6,5}$ (8.0), $J_{6,5'}$ (8.0), $J_{2,3}$ (3.6), $J_{2,3'}$ (3.6)
C_{3x}–Br **8**	1.67–1.93 (m, 3 H), 2.05 (ddd, 3.6, 8.0, 15, H_2), 2.13 (m, 1 H) 2.37 (ddd, 5.4, 9.0, 15.2 H_2), 3.27 (ddd, 6.2, 8.6, 11.7, H_6), 3.38 (td, 8.4, 12, H_1), 4.32 (tt, 3.8, 6.0, H_3), 8.12 (NH)	$J_{1,2}$ (9.0), $J_{1,2'}$ (8.0), $J_{1,6}$ (12), $J_{2,3}$ (5.4), $J_{2',3}$ (3.6), $J_{3,4}$ (3.8), $J_{3,4'}$ (6.0), $J_{5,6}$ (8.6), $J_{5',6}$ (6.2)
C_{3n}–Br **9**	1.78 (m, 3 H), 2.13 (m, 2 H), 2.64 (ddd, 4.5, 7.8, 13.6, H_2), 3.16 (m, H_1 and H_6), 3.78 (tdd, 4.3, 9.0, 11, H_3), 8.23 (NH)	$J_{3,2}$ (4.5), $J_{3,2'}$ (11), $J_{3,4}$ (4.3), $J_{3,4'}$ (9.0), $J_{1,2}$ (7.8)
amide[c] **10**	0.97 (1 H), 1.66 (4 H), 1.88 (1 H), 2.10 (1 H), 2.32 (1 H), 3.01 (1 H), 3.54 (1 H), 5.63 (NH_2)	

[a] $CDCl_3$ solutions with a Me_4Si internal standard were used for recording and decoupling experiments. [b] C_1–Br was obtained as a 1:1 mixture with C_{2x}–Br: the higher field signals are overlapped with those of C_{2x}–Br isomer and could not be resolved. [c] One isomer of **10**.

Table VI. ^{13}C NMR Parameters

compd	chemical shifts, ppm
C_1–Br + C_{2x}–Br[a] **6 + 7**	18.13 (?),[c] 18.92 (t), *20.04* (t), *20.64* (?),[c] 29.57 (t), *32.00* (t), 34.07 (t), *43.36* (d), *43.79* (d), *51.22* (d), 56.26 (d), *62.95* (s), 65.96 (s), *67.58* (s), 67.75 (s), 74.86 (s), 169.55 (C=O), *170.05* (C=O), *170.57* (C=O) (two overlapped signals)
C_{2x}–Br **7**	20.05 (t, C_4), 20.88 (t, C_5), 32.1 (t, C_3), 43.41 (d, C_2), 43.76 (d, C_6), 51.29 (d, C_1) [63, 67.5, 170, 170.5][d]
C_{3x}–Br **8**	19.64 (t), 30.55 (t), 31.90 (t), 39.86 (d), 40.77 (d), 46.35 (d), 67.34 (s), 68.05 (s), 170.35 (C=O), 170.45 (C=O)
C_{3n}–Br[b] **9**	21.64 (t), 33.24 (t), 35.15 (t), 39.74 (d), 43.5 (d), 46.30 (d), 67.19 (s), 69.87 (s), 171.4 (C=O), 171.3 (C=O)
imide **1**	20.8 (t), 21.45 (t), 41.69 (d), 68.04 (s), 171.46 (C=O)

[a] The italic figures are due to the signals of C_{2x}–Br. [b] The spectra was recorded in acetone-d_6; other spectra were recorded in $CDCl_3$. [c] Multiplicity could not be determined. [d] These signals were much weaker than others.

Table VII. IR Absorptions (cm^{-1})

C_{2x}–Br **7**	3240 (m), 3100 (w), 1795 (m), 1735 (s), 1260 (w), 1160 (m), 1150 (m), 1080 (m), 985 (m), 740 (m), 690 (w)
C_{3x}–Br **8**	3350 (m, br), 1790 (m), 1730 (s), 1330 (m), 1260 (w), 1200 (w), 1080 (m), 745 (m)
C_{3n}–Br **9**	3200 (m), 3090 (w), 1790 (m), 1735 (s), 1200 (m), 1160 (m), 1080 (m), 970 (m), 890 (w), 740 (m)
amide[a] **10**	(CH_2Cl_2) 3510 (m), 3400 (m), 1750 (m), 1710 (s), 1590 (m), 1365 (m), 1180 (w), 880 (w), 830 (w)

[a] Except this compound, all others were taken as Nujol mulls.

Table VIII. Mass Spectral Data [*m/e* (%)]

C_1–Br **6**	(EI) 294 (7), 292 (28), 290 (22), 212 (38), 210 (93), 81 (100)
	(CI, CH_4) 332 (6), 330 (46), 328 (100), 326 (65), 294 (3), 292 (10), 290 (8), 250 (14), 248 (50), 246 (63), 214 (20), 212 (68), 210 (42), 205 (27), 203 (39), 178 (20), 176 (25), 170 (24), 168 (54), 166 (38)
C_{2x}–Br **7**	(EI) 294 (2), 292 (8), 290 (6), 212 (38), 210 (100), 171 (6), 169 (27), 167 (39), 81 (26), 80 (18), 79 (23), 77 (18)
	(CI, CH_4) 332 (6), 330 (45), 328 (99), 326 (62), 294 (3), 292 (6), 290 (4), 250 (9), 248 (46), 246 (74), 214 (27), 212 (100), 210 (66), 178 (8), 176 (16), 170 (33), 168 (51)
C_{3x}–Br **8**	(EI) 294 (6), 292 (20), 290 (16), 248 (7), 246 (10), 212 (33), 210 (100), 171 (3), 169 (22), 167 (32), 142 (5), 140 (14), 81 (17), 80 (38), 79 (33), 77 (15)
	(CI, CH_4) 332 (6), 330 (47), 328 (100), 326 (65), 294 (6), 292 (11), 290 (6), 250 (13), 248 (66), 246 (96), 212 (19), 210 (83), 170 (31), 168 (50)
C_{3n}–Br **9**	(EI) 294 (2), 292 (10), 290 (16), 250 (2), 248 (20), 246 (26), 212 (36), 210 (100), 170 (14), 169 (20), 168 (24), 167 (34), 166 (12), 141 (9), 139 (14), 80 (26), 79 (34)
	(CI, *i*-C_4H_{10}) 332 (8), 330 (45), 328 (100), 326 (64), 250 (6), 248 (22), 246 (30)
amide **10**	(EI) 268 (10), 266 (40), 264 (30), 230 (8), 228 (8), 224 (6), 222 (44), 220 (71), 186 (14), 184 (32), 178 (23), 176 (30), 105 (100), 77 (98), 79 (60), 44 (52)
	(CI, CH_4) 306 (0.8), 304 (6), 302 (14), 300 (9, $M^+ + 1$), 268 (2), 266 (8), 264 (6), 216 (6), 214 (19), 188 (30), 186 (100), 150 (15)
amide **10**	(EI) 268 (9), 266 (40), 264 (28), 224 (10), 222 (65), 220 (99), 186 (30), 184 (81), 148 (42), 134 (34), 132 (100), 105 (66), 44 (10)
	(CI, *i*-C_4H_{10}) 306 (7), 304 (46), 302 (100), 300 (62, $M^+ + 1$), 188 (12), 186 (40)

Quantum Yield Determinations. Pyrex test tubes (12 mm × 100 mm length) carrying appropriate solutions were placed in a merry-go-round which was immersed in a water bath kept at 18 ± 2 °C. The light source was a 450-W lamp housed in a Pyrex cooling jacket. The light intensity (5.63×10^{-7} einstein/min) was determined with benzophenone–benzhydrol actinometry ($\Phi = 0.74$ in benzene) as described before.[9]

A stock solution of **2** (102.2 mg, 0.314 mmol) and methylene chloride (50 mL, 6.3×10^{-3} M) was prepared. To each phototube, 3-mL aliquots were charged and degassed with argon for ca. 5 min. Irradiation of the solution under these conditions developed light yellow color in about 10 min. At suitable intervals, an irradiated tube was removed. To the solution, one drop of *tert*-butylethylene was added to trap bromine. The solution was added to 10 mL of KI solution (5 g of KI in 250 mL of water and 150 mL of glacial acetic acid). This mixture was analyzed by iodometry using $Na_2S_2O_3$ solution (2×10^{-3} N) for titration. Blank experiments were also carried out to make corrections on the titrations.

In a separate series of experiments, the *N*-bromide stock solution (3 mL) and a bromine solution (0.05 mL, 0.04 M) were added to tubes. These solutions were purged with argon for 5 min at 0 °C and were irradiated. The treatment of the solutions and analysis followed the same procedures as that shown above. A series of similar solutions was irradiated through a GWV filter and analyzed in the same way using ferrioxalate actionometry.[10]

In separate experiments, to each tube charged with 3 mL of the stock solution of **2**, *tert*-butylethylene (5 μL, 0.04 mmol) was added. These tubes were irradiated and analyzed as above, except that *tert*-butylethylene was not added after photolysis.

Acknowledgment. We are much indebted to the Natural Sciences and Engineering Council of Canada for generous support of this project. We thank Professor P. S. Skell most sincerely for his valuable comments.

Registry No. 1, 91949-21-2; **2**, 91949-22-3; **3**, 91949-23-4; **6**, 91949-24-5; **7**, 91949-25-6; **8**, 92075-87-1; **9**, 91949-26-7; **10** (isomer 1), 91949-27-8; **10** (isomer 2), 92075-88-2.